J Mater Sci (2008) 43:7230–7238
DOI 10.1007/s10853-008-2938-x

Mechanical and tribological behavior of clay–polypropylene nanocomposites

K. Kanny · P. Jawahar · V. K. Moodley

Received: 26 March 2007 / Accepted: 6 August 2008 / Published online: 20 September 2008

Abstract This study deals with the wear rates and quasi-static mechanical properties of polypropylene (PP) infused with layered organo-modified montmorillonite nanoclays. Test results show that PP infused with 2 wt.% of organo-modified montmorillonite gives improved mechanical strength, higher fracture toughness, and lower wear rates. Transmission electron microscopy shows that the structure of the modified nanocomposite changes from an exfoliated structure at 1 wt.% nanoclay loading to an intercalated structures at 5 wt.% nanoclay loading. The general improvement in properties, which includes but not limited to the thermal barrier properties, may be attributed to the change in structure.

Introduction

Researchers continue to show increased interest in the study of polymer-layered silicate nanocomposites mainly because these nanocomposites exhibit a wide range of improved properties after modification [1]. Many nanofillers and compatibilizing agents have been used successfully in the synthesis of these nanocomposites. New synthesizing techniques such as the melt blending technique, in situ polymerization, and melt intercalation have been used to develop different materials systems [2]. The substantial improvements in mechanical, thermal, and physical properties of polymer-layered silicate nanocomposites have widen the use of these polymers in industry. In the late 1980s, the Toyota Motor Company commercialized a timing belt cover made from nylon-6/nanoclay composites for one of its car models demonstrating that thermoplastic nanocomposites are one of the most promising materials for usage in domestic and industrial applications [3]. More recently researchers Kojima et al. [4] and Kato et al. [5] showed that for nylon-6 (N6)/MMT nanocomposites very small amounts of layered silicate loadings, approximately <5 wt.%, resulted in pronounced improvements of thermal and mechanical properties. These findings are in agreement with findings in our study.

Effective dispersion of the nanoclays within the polymer matrix results in enhancing the mechanical properties. Morphological analyses of these structures reveal that they can be categorized into three general types: a conventional composite where the nanoclay acts as conventional filler, intercalated nanocomposite which consists of a regular insertion of polymer between the silicate layers, and exfoliated nanocomposite where 1-nm thick silicate layers are dispersed within the polymer matrix [3, 6]. These types of nanocomposite structures are shown in Fig. 1.

Bharadwaj et al. suggest that the mechanical properties of a virgin polymer are enhanced when exfoliation occurs with extremely low concentrations of nanoclays (1–3 wt.%) as compared to conventional phase-separated composites of a filler material in a polymer. The large surface area available for interactions with the polymer matrix coupled with high aspect ratio is responsible for the enhancement in properties [7] (Fig. 2).

Similarly, in a recent study we have found substantial improvements in the mechanical properties of a nanophased composite at low weight percentages (0.5–2 wt.%) [8]. The mechanical properties improved with an increase in nanoclay loading up to a threshold of 2 wt.%; thereafter, the material properties degraded. This improvement was

K. Kanny (✉) · P. Jawahar · V. K. Moodley
Department of Mechanical Engineering, Durban University of Technology, Durban 4001, South Africa
e-mail: kannyk@dut.ac.za

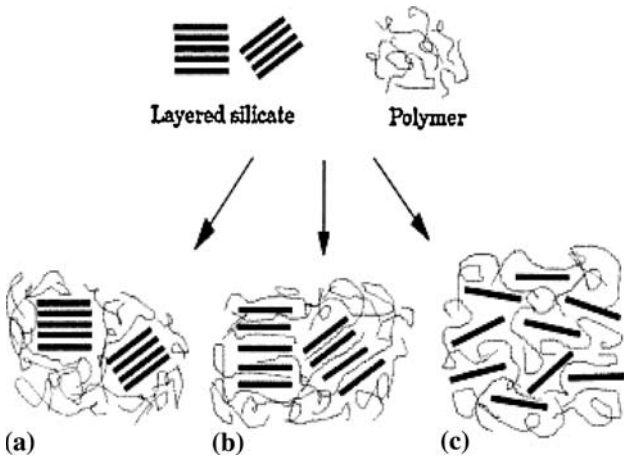

Fig. 1 Types of polymer-layered silicate composites [1]. (**a**) Phase separated (microcomposite), (**b**) intercalated (nanocomposite), and (**c**) exfoliated (nanocomposite)

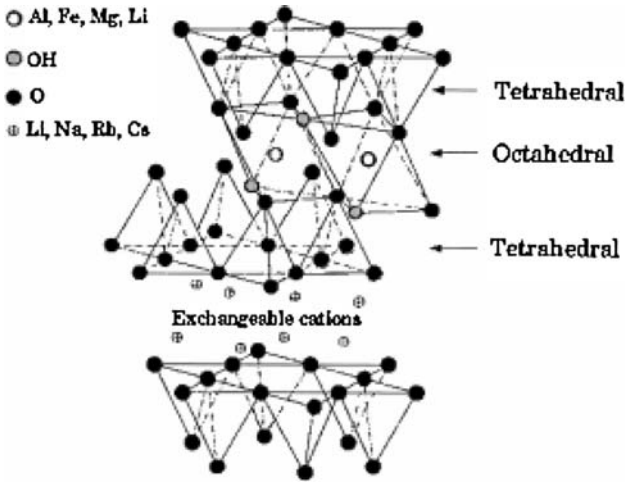

Fig. 2 Structure of 2:1 phyllosilicates (MMT, Hectorite, Saponite) [3]

coupled with a trend in which the material tends to harden [8, 9]. The hardening effect suggests that the material may be used as a bearing surface; however, its thermal barrier and tribological properties needs to be evaluated.

The authors take cognizance of the fact that previously the incorporation of nanosize particles like titanium dioxide (TiO_2) [10], silicon oxide (SiO_2) [11], zirconium oxide (ZrO) [12], silicon carbide (SiC) [13], silicon nitride (Si_3N_4) [14], and aluminum oxide (Al_2O_3) [15, 16] to a polymer matrix has lead to enhancement in wear resistance. It is expected that incorporation of organoclays at nano-level will also improve the wear properties of nanocomposites.

In this study, the influence of nanoclay addition to a polypropylene (PP) matrix on the tribological properties needs to be evaluated. The thermal barrier properties, compression behavior, fracture toughness, and storage modulus of clay–polypropylene nanocomposites are also investigated.

Experimental

Materials and preparation of nanocomposite specimens

Nanophased thermoplastic composite structures were prepared by infusion of Cloisite®15A nanoclays (Southern Clay Products, Gonzales, TX, USA) into a polypropylene matrix (COSMOPLENE®Y101E, CHEMPRO, SA) using the melt blend technique. Polypropylene pellets were heated to its melt temperature, 170 °C (see Table 1), in a LABCON HTR2 environmental chamber.

To avoid thermal shock, the temperature was ramped up by 10 °C/min to a maximum temperature of 170 °C. Upon reaching 170 °C, the material was left in the oven at the set temperature to effect temperature soaking. The temperature was measured using a TESTO QTA25-T4 PYROMETER temperature probe with the LABCON HTR2 digital display. The plastic surface and chamber temperature was measured accurately within a ±2 °C range thus allowing successful control of temperature ramping. The mixtures were vigorously blended using a paddle stirrer for approximately 3 min. A very viscous homogenous molten plastic at melt temperature was then carefully poured into a specially manufactured mold. The molten plastic was then cast into the molds at point A (see Fig. 3) at point A. The liquid plastic then flows into the shaped mold cavity forming the specimens. Air holes are provided to minimize

Table 1 Properties of COSMOPLENE®Y101E POLYPROPYLENE

Item	Unit	Y101E	ASTM method
Melt flow rate	g/10 min	17	D1238
Density	g/cm^3	0.90	D1505
Tensile strength at break	kg/cm^3	350	D638
Elongation	%	>600	D638
Flexural modulus	kg/cm^2	14,000	D790
Izod impact strength	kg cm/cm	2.0	D256
Melting point	°C	165	N/A

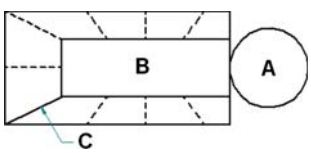

Fig. 3 Schematic of specimen mold designed with air holes. A: Pour pot (depth = 12 mm), B: net shapped mold (depth = 10 mm), and C: bleed holes

any air entrapments as shown in Fig. 3. The specimen is then allowed to cure at room temperature. Test coupons were then machined from these panels.

A similar technique was employed to manufacture the nanophased structures except the temperature was ramped at 10 °C/min to 185 °C. The higher temperature setting was used to produce a less viscous polymer matrix to enable better nanoclay dispersion via blending. The increase in temperature rendered the molten plastic to be less viscous thus enabling an easier mixing process. At this stage Cloisite®15A nanoclays measured in specific weight percentages 0.5; 1; 2; 3; and 5 were added to separate batches of the molten plastic.

Nanocomposite characterization

X-ray diffraction patterns were obtained using a Philips PW1050 diffractometer using monochromated Co-$K\alpha$ radiation. ($\lambda = 0.1788965$ nm, 40 kV, 120 mA) at room temperature. The diffractograms were scanned from 2.5° to 10° (2θ) in steps of 0.02° using a scanning rate of 0.5°/min. X-ray diffractograms were taken on closite 15A clay and polypropylene composites containing 0.5, 1, 2, 3, and 5 wt.% closite 15A nanoclay to confirm the formation of nanocomposites on addition of organoclay.

Microscopic investigation of selected nanocomposite specimens at the various weight compositions were conducted using a Philips CM120 BioTWIN transmission electron microscope with a 20–120 kV operating voltage. The cryo and low dose imaging TEM has BioTWIN objective lens that gives high contrast and a resolution of 0.34 nm. The microscope is equipped with an energy filter imaging system (Gatan GIF 100) and digital multiscan CCD cameras (Gatan 791). The specimens were prepared using a LKB/Wallac Type 8801 Ultramicrotome with Ultratome III 8802A Control Unit. Ultra thin transverse sections, approximately 80–100 nm in thickness were sliced at room temperature using a diamond knife. The sections were supported by 100 copper mesh grids sputter-coated with 3 nm thick carbon layer.

Quasi static mechanical tests

Compression tests on the nanocomposite specimens were performed using the Lloyds Tensile Tester fixed with a 20 kN load cell. The compression testing was carried out on specimens with dimensions of $15 \times 8 \times 8$ mm^3 in accordance with the ASTM D 3410-87 testing standard [17].

The Vickers hardness of the virgin and nano-infused polypropylene specimens was determined using a Matsuzawa DMH2 microhardness tester. Specimens of dimension $14 \times 12 \times 6$ mm^3 were indented with a 100-gf load for a period of 5 s. The diagonals of the indentation were measured and the Vickers hardness was automatically computed and read of a digital display.

Five specimens from each weight percent category were subjected to the above tests.

Fracture toughness

The stress intensity factor (K_{IC}) and the strain energy release rates (G_{IC}) for virgin and nanocomposite specimens were determined using the single-edge notch bending specimen (SENB). A minimum of five specimens were tested for each weight category of virgin PP and nano-infused PP structures. The specimens were prepared in accordance with the ASTM D5045-93 testing standard [18]. Specimens with dimensions $125 \times 25 \times 6$ mm^3 were notched to a depth of 5 mm with a thin saw blade and a grid was plotted on the front view of the specimen to observe the crack propagation. The LLOYDS tensile testing machine fixed with a 20-kN load and fitted with a three-point bend fixture was used to conduct the tests.

Dynamic mechanical analysis

Dynamic mechanical analysis (DMA) was performed using dynamic mechanical analyzer (Netzsch DMA 242C) in the three point bending mode at a frequency of 10 Hz over the temperature range of 20–120 °C at a heating rate of 2 °C/min. DMA was performed primarily to determine the storage modulus of PP and nanocomposite samples at the different temperatures indicated and at the glass transition temperature (T_g).

Tribological testing

Pin-on-disc wear test was carried out, using locally manufactured tribometer, in accordance with ASTM G-99 standard [19]. It consists of a loading disk, where loads are kept, and applied over the square pins. The dimension of the wear test pins is 8 mm square and 20 mm in length. The disc used was brass of surface roughness 0.2 μm. The specific wear rate of the conventional composites and nanocomposites was determined at a constant contact pressure of 0.15 MPa and sliding velocity of 0.35 m/s for the sliding distance of 3600 m. Wear tracks of pins was observed using ZEISS AXIO LAB optical microscope.

Results and discussion

X-ray and TEM characterization

XRD pattern of closite 15A (CL15A) clays and of clay–polypropylene nanocomposites are shown in Fig. 4. The

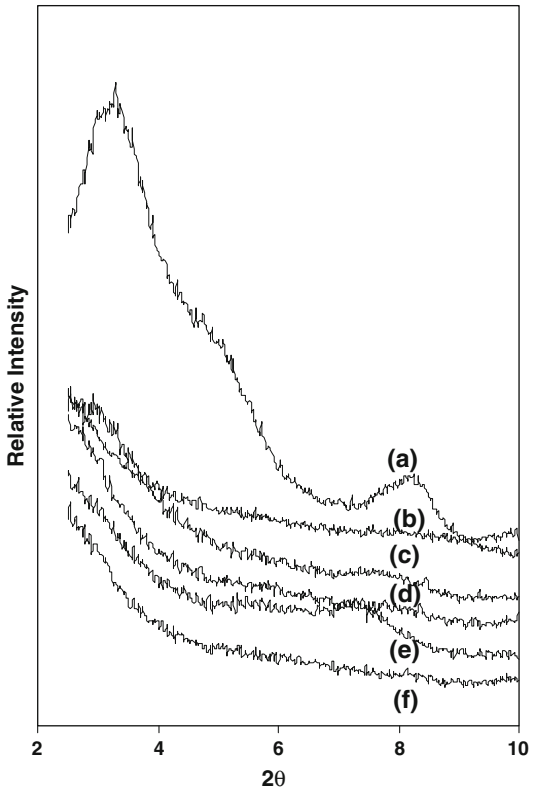

Fig. 4 X-ray diffraction pattern of (a) CL15A and PP with (b) 0.05 wt.% CL15A, (c) 1 wt.% CL15A, (d) 2 wt.% CL15A, (e) 3 wt.% CL15A, and (f) 5 wt.% CL15A

closite 15A shows a distinct peak at the 2θ value of 3.3° and the corresponding initial intergallery spacing is 31.09 Å. No distinct peaks were found in the polypropylene nanocomposites containing different weight fractions of closite 15A. During mixing the polymer infuses and intercalates between the intergallery spacing of layered silicates and separates the clay layers gradually. The disappearance of peak indicates the separation of clay layers and the formation of intercalated or exfoliated nanocomposite. The final confirmation can be achieved only by analyzing transmission electron micrographs pictures.

Transmission electron microscope pictures were taken on nanocomposite samples with 1 and 5 wt.% nanoclay to compare with the XRD pattern. In the analysis of PP with 1 wt.% nanoclay, the TEM images shows that the nanoclay dispersed well and the clay platelets were regularly intercalated and exfoliated (Fig. 5a). This confirms that the PP with 1 wt.% nanoclay has exfoliated and intercalated as represented by the XRD figures (Fig. 3). The PP with 5 wt.% nanoclay displays a different behavior (Fig. 5b). The clay platelets are closely packed compared to the PP nanocomposites with 1 wt.% nanoclay. It resembles intercalated structure. This confirms that incorporation of nanoclays to the polypropylene matrix leads to the formation of intercalated and exfoliated nanocomposites for lower clay concentration (1 wt.%) and intercalated nanocomposites for higher clay concentration (5 wt.%).

Both micrographs also show black circular (porous) regions which result from air entrapments during the manufacturing process and may influence the properties of the composites.

To evaluate the influence of the porosity, a detailed study was undertaken.

In this study the porosity index is defined as,

$$\phi = \frac{V_V}{V_T} \tag{1}$$

where ϕ denotes the porosity index. V_V is the volume of void-space (air entrapments) and V_T is the total volume of material of each sample. V_V is obtained by determining the total volume of the black circular spots on each micrograph at each weight percentage. V_T is obtained by calculating the total volume of the specimen. Table 2 shows the porosity index for all samples.

The results shown in Fig. 6 indicate that the porosity index of 0.5, 1, 2, 3, and 5 wt.% PP-CL 15A nanosections are fairly consistent.

Compression testing

The compression stress–strain curves for the virgin PP and nanocomposites are shown in Fig. 7. Comparison of the

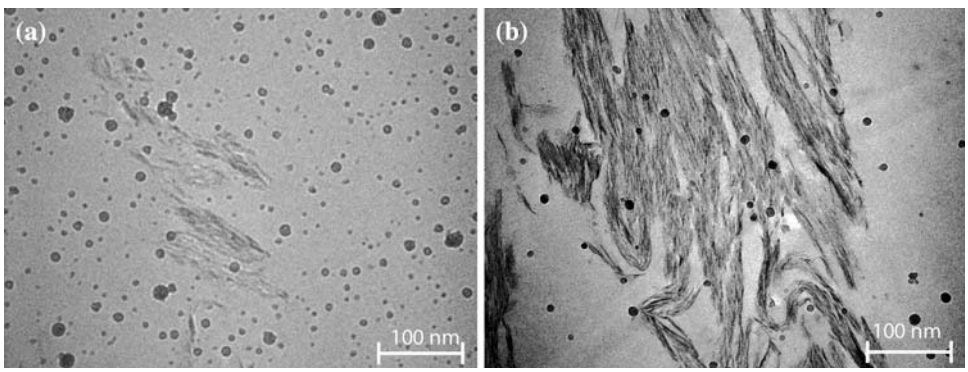

Fig. 5 Transmission electron micrographs of nanocomposites with (**a**) 1 wt.% CL15A and (**b**) 5 wt.% CL15A

Table 2 Porosity of polypropylene Cloisite®15A nanocomposites

Specimen	Clay content, wt.%	Average volume (voids), V_v, μm^3	Average volume (slice), V_T, μm^3	ϕ (V_V/V_T) %
PP 005CL15A	0.5	0.00018757	0.00839151	2.24
PP0CL15A	1	0.00023690	0.03356602	0.71
PP02CL15A	2	0.00023497	0.03356602	0.70
PP03CL15A	3	0.00004606	0.00415247	1.11
PP05CL15A	5	0.00006690	0.00415247	1.61

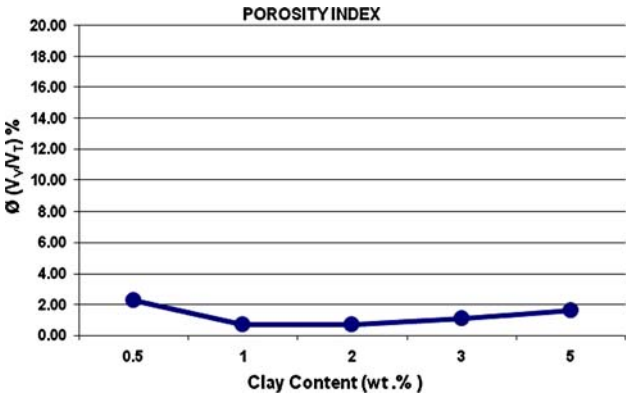

Fig. 6 Porosity index of clay polypropylene nanocomposite

Table 3 Compressive properties of polypropylene Cloisite®15A nanocomposites

Specimen	Clay content, wt.%	Average modulus, GPa	Average compressive strength, MPa
PP-neat	0	1.1	44
PP005CL15A	0.5	1.3	47
PP01CL15A	1	1.4	49
PP02CL15A	2	1.5	54
PP03CL15A	3	1.5	57
PP05CL15A	5	1.6	58

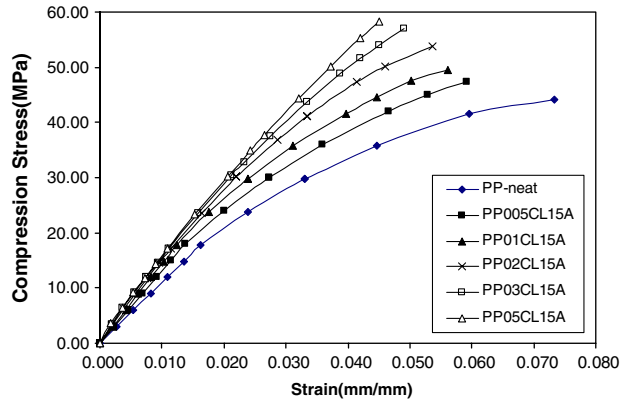

Fig. 7 Compression stress–strain curves of clay polypropylene nanocomposite

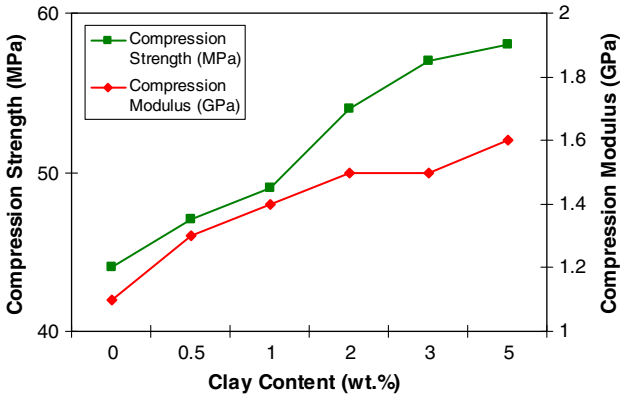

Fig. 8 Compression strength and modulus for clay–polypropylene nanocomposites

slopes of the virgin and nanocomposite structures in the elastic region indicates an increase in gradient. This increase in slope suggests an increase in the material stiffness with an increase in nanoclay loading up to 5 wt.%. Figure 7 shows the compression modulus and compressive strength as a function of clay concentration.

The compression strength and modulus for virgin and infused polypropylene is shown in Table 3.

The compression strength of polypropylene is 44 MPa. There is a gradual increase in compressive strength from 44 MPa for virgin polypropylene to 58 MPa for 5 wt.% infused specimens. Similarly, the compression modulus of virgin polypropylene is 1.1 GPa. It increases to 1.6 GPa for polypropylene infused with 5 wt.% nanoclays. This trend is shown in Fig. 8.

The addition of nanoclay significantly increases the compression strength and compression modulus of virgin PP by 32% and 45%, respectively. This improvement is due to the presence of intercalated and exfoliated clay platelets as seen in the TEM images of PP nanocomposites. This is consistent with the findings of Chang et al. [20]. The nanoclay is intercalated by the PP polymer chains and confines the segmental movement of the PP macromolecules resulting in increased compressive modulus.

Fracture toughness

SENB tests were performed on virgin and polypropylene nanocomposites with different weight percentages of clay and the resistance to crack propagation was measured. The stress intensity factor (K_{IC}) and strain energy release rate (G_{IC}) of virgin polypropylene and clay polypropylene nanocomposites is shown in Fig. 9.

The stress intensity factor (K_{IC}) and strain energy release rate (G_{IC}) of virgin polypropylene is 2.00 MPa $m^{1/2}$ and 1765 J/m^2 (Table 4).

The stress intensity factor and strain energy release rate increased with the addition of nanoclays. The nanocomposites exhibits a maximum improvement in K_{IC} and G_{IC} for the clay content of 5 wt.%. This improvement in the K_{IC} and G_{IC} values is due to the presence of the intercalated nanoclay structures in the polypropylene nanocomposite structure that act as load-bearing agents, and also acts as crack stopping agents. The intercalated dispersion of the clay platelets prevents the easy propagation of the crack by allowing the crack to propagate through torturous pathway resulting in increased fracture resistance and also increases the stress intensity factor and strain energy release rate of the polypropylene nano-infused specimens.

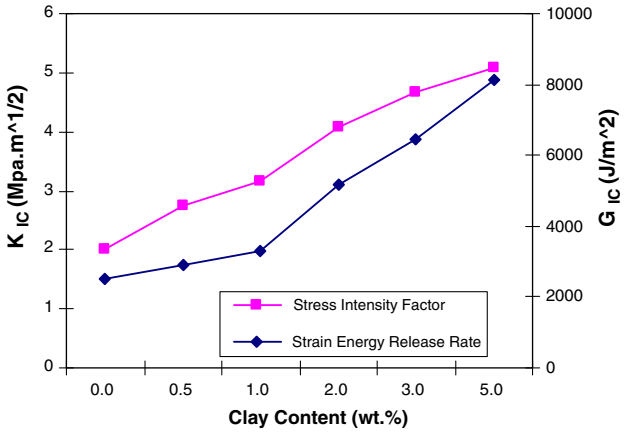

Fig. 9 Stress intensity factor (K_{IC}) and strain energy release rates (G_{IC}) for nanocomposite specimens

Table 4 Stress intensity factor (K_{IC}) and strain energy release rates (G_{IC}) for nanocomposite specimens

Specimen	Clay content, wt.%	Average K_{IC}, MPa $m^{1/2}$	Average G_{IC}, J/m^2
PP-neat	0	2.00	2502
PP005CL15A	0.5	2.75	2925
PP01CL15A	1	3.17	3298
PP02CL15A	2	4.09	5191
PP03CL15A	3	4.67	6429
PP05CL15A	5	5.09	8106

Hardness of nanocomposites

The hardness of neat PP and nanocomposites were shown in Fig. 10. The hardness of the nanocomposites gradually increases with increasing clay content. PP05CL15A specimens displayed the largest hardness numbers averaging at 13.6. The reason for the improvement in the hardness is due to the presence of intercalated and exfoliated clay platelets present in the polypropylene matrix. The intercalated/exfoliated clay platelets effectively restrict indentation and increase the hardness of the nanocomposites [21]. The improvement in hardness can be corroborated to the improvement in compression modulus of nanocomposites with increase in organoclay.

Dynamic mechanical analysis

The storage modulus E' at different temperatures for neat PP and PP infused with different weight fractions of closite 15A is shown in Fig. 11.

The storage modulus (E') of neat PP at 20 °C is 1450 MPa. The E' of specimens infused with 3 and 5 wt.% is 1750 and 1500 MPa, respectively. At 20 °C, the E' of PP has an increasing trend up to a weight percentages of

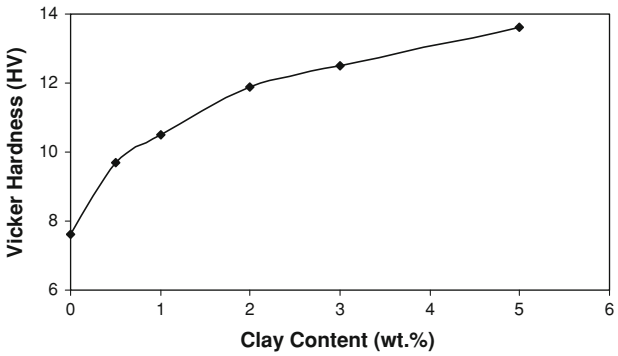

Fig. 10 Hardness of clay polypropylene nanocomposites

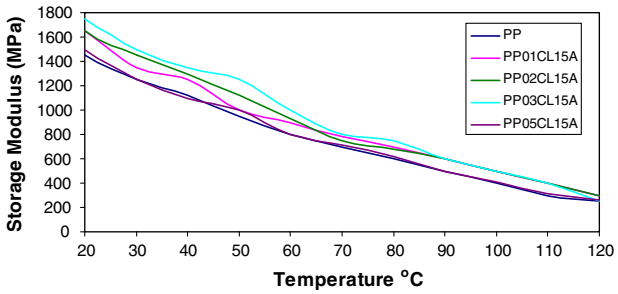

Fig. 11 Storage modulus of neat PP and clay–PP nanocomposites

nanoclays at 3 wt.%. At higher nanoclay weight percentages of 5 wt.%, the E' decreases. This scenario is plausible because at higher clay contents, clay structures remain as microtactoids contributing to the deterioration of the storage modulus. It was evident from DMA curves, that the nanocomposite samples exhibit a better E' than virgin PP.

The loss factor curve shows the glass transition temperature (T_g) of the virgin PP and the nanocomposite samples (Fig. 12).

The glass transition temperature is obtained from the corresponding peak values of the loss factor curve. The peaks in tan δ curves correspond to the glass transition temperature (T_g). It is evident from loss factor curve that there is a significant increase in the glass transition temperature from 70 °C for PP to 109 °C for PP reinforced with 3 wt.% of clays. The improvement in T_g may be attributed to the presence of nanoclays which reduces the mobility of the crystals in the amorphous phase of the PP matrix.

Tribology testing

The specific wear rate of virgin PP and the nanocomposite samples is shown in Fig. 13.

The specific wear rate of neat PP is $4.27e^{-4}$ mm^3/N m and decreases with the infusion of nanoclays at all the weight loadings. The specific wear rate of PP with 2 wt.% nanoclays decreases to $6.43e^{-05}$ mm^3/N m while the wear loss of PP with 5 wt.% nanoclays decreases to $1.26e^{-04}$ mm^3/N m. Nanocomposites with 2 wt.% nanoclay show a maximum of 85% improvement in wear resistance. The improvement in wear resistance is mainly attributed to the presence of clay platelets in the PP matrix. These nanosize clay platelets dispersed in the polymer matrix act as a barrier and also prevent large-scale fragmentation of the polymer matrix. The nanoclay platelets dispersed in the polypropylene matrix lead to interfacial strengthening and increased wear resistance [22, 23]. The high interfacial adhesion between the matrix and nanoclay is due to the high specific surface area of the nanoparticles. The nanoparticle having the same size as the segments of the surrounding polymer chains enables the material removal to be mild and aids the formation of uniform tenacious transfer film as reported elsewhere [24, 25]. Hardness contribution also plays a vital role in wear property improvement as reported elsewhere [26].

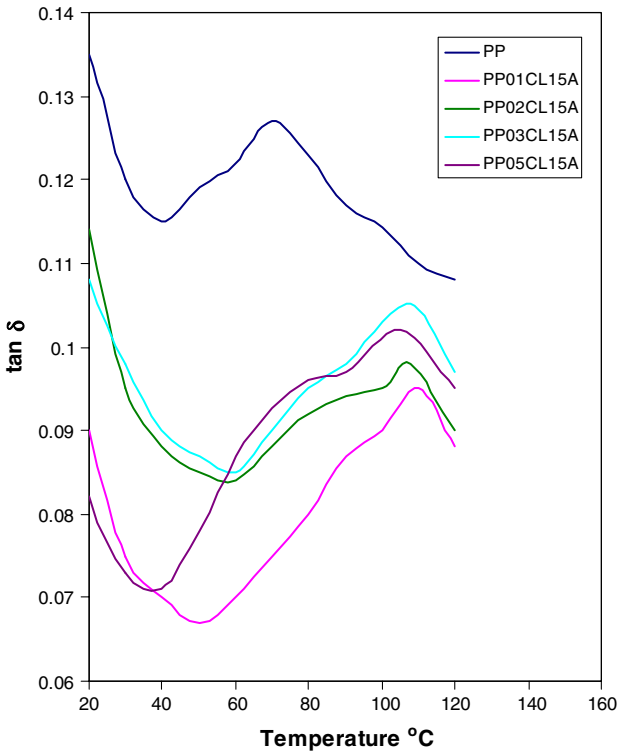

Fig. 12 Loss factor curve of neat PP and clay–PP nanocomposites

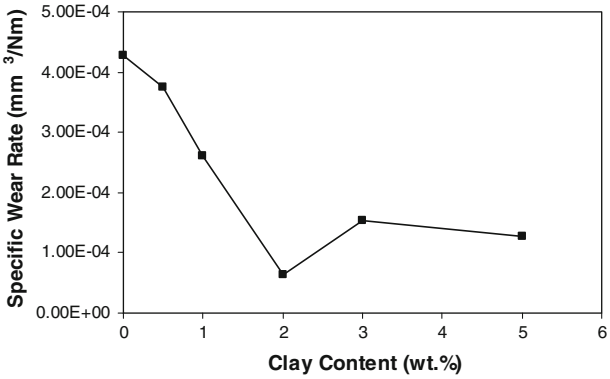

Fig. 13 Wear loss of neat PP and nanocomposites

The wear tracks of neat polypropylene and clay polypropylene nanocomposites were analyzed. The wear track of neat polypropylene is smooth with some deep ploughing marks as shown in Fig. 14. The mode of material removal

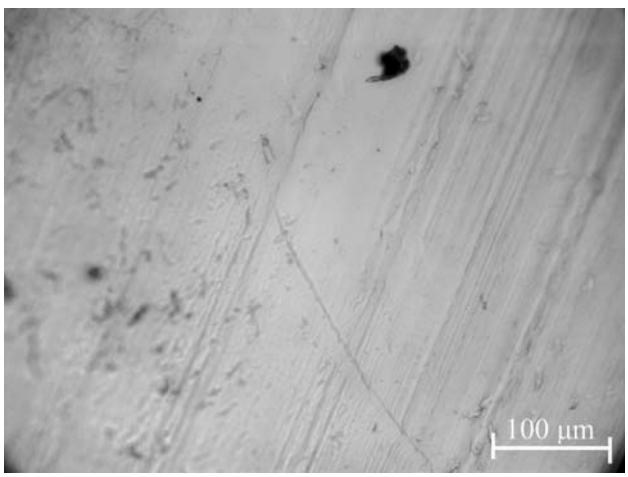

Fig. 14 Wear surface of neat polypropylene

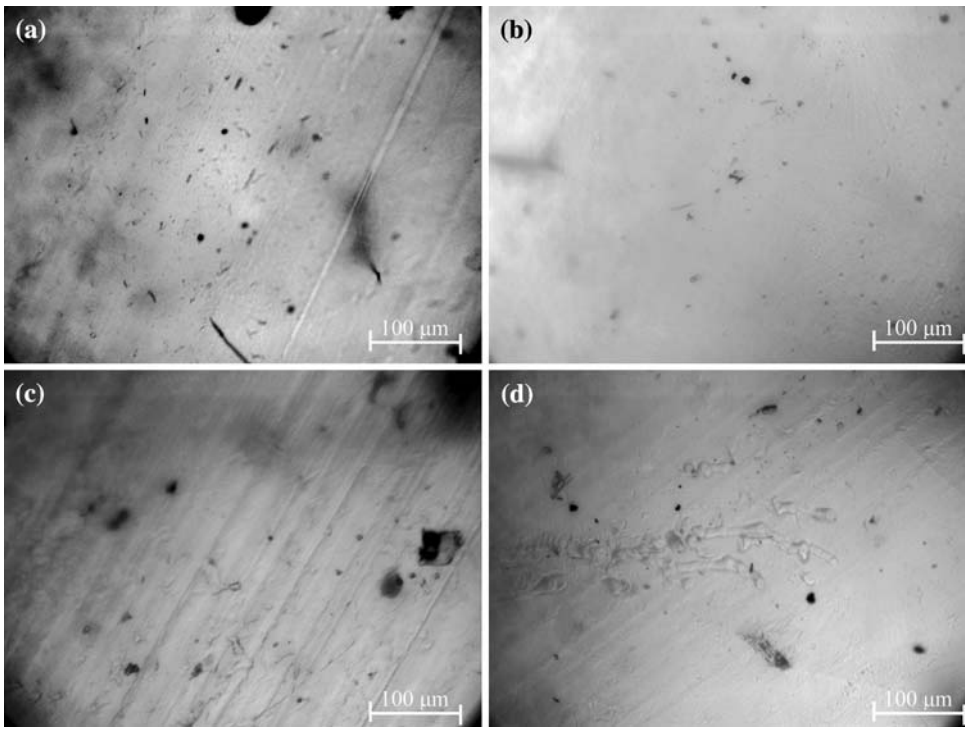

Fig. 15 Wear surfaces of clay polypropylene nanocomposites with (**a**) 0.5 wt.% CL15A, (**b**) 2 wt.% CL15A, (**c**) 3 wt.% CL15A, and (**d**) 5 wt.% CL15A

is by the ploughing action of the hard asperities of the brass counter disk when the surface of the polypropylene pin slides over the counter face. As neat polypropylene is soft, the asperity in the brass counter face acts as cutting edge and ploughs the material surface and removes the material as wear debris.

The optical micrograph shows the wear tracks of nanocomposite samples (Fig. 15). The wear mechanism is similar in nanocomposite samples. The material is removed from the surface of the nanocomposite test pins by the ploughing and cutting action of asperities allowing the wear surfaces of the nanocomposites test pins with 0.5, 1, and 2 wt.% clay loadings to be smooth. Analysis of the experimental results indicates that the nanocomposite pins infused with 2 wt.% nanoclay is smooth (glassy) and it has better wear resistance than the neat PP and other nanocomposite specimens. The wear tracks of nanocomposites with 3 and 5 wt.% are comparatively rougher than other nanocomposite samples. Moreover, the optical picture for nanocomposites with 5 wt.% nanoclay shows some patches on the surface. The agglomerated clay might have pulled out of the sliding surface and the pulled out regions remains as patch.

The nanocomposites with 2 wt.% nanoclay have shown the best wear resistance. The adhesion between the matrix and the intercalated nanoclay platelets is good and leads to the better resistance for nanocomposite samples. The dispersed intercalated nanoclay also is suggestive of leading to the better adhesion between the films on the counter face as reported elsewhere [27, 28]. Further studies needs to be completed to analyze the counter face and to have an improved understanding of the wear behavior of nanocomposite.

Conclusions

1. The nanocomposite samples show a maximum improvement of 31% and 45% in compression strength and compression modulus, respectively, for the nanoclay content of 5 wt.%.
2. The incorporation of nanoclay significantly improves the stress intensity factor (K_{IC}) and strain energy release rate (G_{IC}) to a maximum of 124% and 137%, respectively, for the clay content of 3 wt.%.
3. The incorporation of nanoclay improves the storage modulus significantly and also increases the glass transition temperature from 70 °C for virgin PP to 109 °C for the nanoclay content of 2 wt.%.
4. The wear resistance of nanocomposite samples increases to a maximum of 85% for 2 wt.% nanoclay.

References

1. Alexander BM, Gilman JW (2003) J Appl Polym Sci 87:1329. doi:10.1002/app.11884
2. Kenny JM, Torre L, Valentini L, Biagiotti J, Puglia D (2002) In: Proceedings of China–EU forum on nanosized technology, Beijing, PR China, December, p 24

3. Alexandre M, Dubois P (2000) Mater Sci Eng 28:1. doi:10.1016/S0927-796X(00)00012-7
4. Kojima Y, Usiki A, Kawasumi M, Okada A, Fukushima Y, Karauchi T et al (1993) J Mater Res 6:1185. doi:10.1557/JMR.1993.1185
5. Kato MY, Usiki A, Okada A (1997) J Appl Polym Sci 66:1781. doi:10.1002/(SICI)1097-4628(19971128)66:9<1781::AID-APP17>3.0.CO;2-Y
6. Utracki LA, Kamal MR (2002) Arab J Sci Eng 27:43
7. Bharadwaj RK, Mehrabi AR, Hamilton C, Trujilo C, Murga M, Fan R et al (2002) Polymer (Guildf) 43:3699
8. Moodley VK, Kanny K (2007) J Eng Mater Technol 40:1
9. Ding C, Jia D, Hui H, Guo B, Hong H (2004) Polym Test 20:1
10. Chang L, Chang Z, Bredit C, Friedrich K (2005) Wear 258:141. doi:10.1016/j.wear.2004.09.005
11. Wang Q, Xue Q, Shen W (1997) Tribol Int 30:193. doi:10.1016/S0301-679X(96)00042-4
12. Wang Q, Xue Q, Shen W, Zhang J (1998) J Appl Polym Sci 69:135. doi:10.1002/(SICI)1097-4628(19980705)69:1<135::AID-APP16>3.0.CO;2-Z
13. Wang Q, Xue Q, Liu W, Chen J (2000) Wear 243:140. doi:10.1016/S0043-1648(00)00432-4
14. Wang Q, Xue Q, Liu W, Chen J (2001) J Appl Polym Sci 79:1394. doi:10.1002/1097-4628(20010222)79:8<1394::AID-APP60>3.0.CO;2-D
15. Sawyer WG, Freudenberg KD, Bhimaraj P, Schadler LS (2003) Wear 254:573
16. Shi G, Zhang MQ, Rong MZ, Wetzel B, Friedrich K (2004) Wear 256:1072. doi:10.1016/S0043-1648(03)00533-7
17. ASTM D 3410-87 (2004) Standard test method for compressive properties of unidirectional or crossply fiber-resin composites. In: ASTM Book of Standards, 08.02, July, Plastics (II), pp D2383–D4322
18. ASTM D5045-99 (2004) Standard test methods for plane-strain fracture toughness and strain energy release rate of plastic materials. ASTM Book of Standards, 08.03, July, Plastics (III), p D4329
19. ASTM 699-05 (2005) Test method for wear testing with a pin-on-disk apparatus (R). ASTM Book of Standards
20. Chang JH, Seo BS, Hwang DH (2002) Polymer (Guildf) 43:2969. doi:10.1016/S0032-3861(02)00125-8
21. Jawahar P, Balasubramanian M (2005) Int J Plast Technol 9:472
22. Cai H, Yan FE, Xue Q, Liu W (2003) Polym Test 22:875. doi:10.1016/S0142-9418(03)00024-2
23. Shi G, Zhang MQ, Rong MZ, Wetzel B, Friedrich K (2004) Wear 256:1072. doi:10.1016/S0043-1648(03)00533-7
24. Wang QH, Xu J, Shen W, Xue Q (1997) Wear 209:316. doi:10.1016/S0043-1648(97)00015-X
25. Shwartz CJ, Bahadur S (2000) Wear 237:261. doi:10.1016/S0043-1648(99)00345-2
26. Khedkar J, Negulescu L, Meletis EI (2002) Wear 252:361. doi:10.1016/S0043-1648(01)00859-6
27. Cheng XH, Xue YJ, Xie CX (2002) Wear 253:869. doi:10.1016/S0043-1648(02)00217-X
28. Bahadur S (2000) Wear 245:92. doi:10.1016/S0043-1648(00)00469-5